SIMULATION AND MEASUREMENT OF VERY FAST TRANSIENT OVERVOLTAGE UP TO 2.5MV

LU ZHANG[1], QIAOGEN ZHANG[1]*, SHI LIU[1], ZHOU LI[1], YU YIN[2], WEIDONG SHI[2], LONG LI[1], FENGLIAN LIU[1], XIN TONG[1], JIN WEI[1], JIAN HUANG[1]
[1] State Key Laboratory of Electrical Insulation and Power Equipment, Xi'an Jiaotong University, Xi'an 710049, China,
[2] China Electric Power Research Institute, Beijing 100192, China
*Email: <hvzhang@mail.xjtu.edu.cn>

Abstract: Very fast transient overvoltages (VFTOs) generated during circuit breakers or disconnector switches operations in ultra high voltage gas insulated switchgears (GIS) make great threats to the insulation of power equipments. For the purpose of more economical of GIS insulation design and insulation co-ordination, it is necessary to research the insulation characteristics of GIS equipments under VFTOs. In this paper, simulation results of designed high voltage circuit using Electro Magnetic Transients Program, a systemic design method of VFTO generation and measurement were proposed. Besides, the effects of circuit configuration on VFTO parameters were also researched. Finally, VFTO generated by the system was measured. Simulation results revealed that the intermediate storage capacitor had a big effect on output efficiency and frequency of VFTO. The inductance of generation circuit should be as small as possible. While resistance should be chosen properly for higher efficiency and proper oscillation of VFTO. Test results demonstrated the newly developed generation system could generate 2.5MV VFTO, which had a risetime of 49ns and oscillation frequency of 8.1MHz. The VFTO generation system can help to better research insulation characteristics of GIS.

1 INTRODUCTION

Gas insulated switchgear (GIS) has been widely used in electrical power systems for decades. Recently, it has also been motivated by the ultra high voltage transmissions in China[1]. Compared with the air insulated substations(AIS), GIS is more reliable, occupies much less space, is not affected by weather and can be aesthetically integrated into the ambient surroundings[2]. However, VFTO is generated during circuit breaker or disconnector switch operations in GIS, which makes great threats to the insulation of power equipments.

Amplitude of VFTO almost increases linearly with the increase of voltage level. For 1000kV GIS, the rated voltage increases almost one time than 500kV GIS. However, the insulation level of it increases only 55% than 500kV GIS. Insulation failures will be more serious in ultra high voltage GIS. So, it is of practical and economical [3] interests to research insulation characteristics of 1000kV GIS equipments under VFTO in laboratory. Although many simulation systems of VFTO in laboratory have been reported [4-7] and many works [6-14] have been done in the field of VFTO, most of the present studies of VFTO amplitude is of several hundred kilovolts, of which the results can't guide the design of GIS directly. In addition, the effects of electrode shapes, voltage polarities and electrode space on the breakdown voltage under ultra high VFTO are lack of systemic research. These requirements call for the development of a new simulation system which can generate VFTO of several megavolts for researching insulation characteristics of GIS.

In this paper, based on simulation results of high-voltage circuit using Electro Magnetic Transients Program (EMTP), each part of generation and measurement system of VFTO was analyzed and selected. Simulation results demonstrated that the intermediate storage capacitor (ISC), the damping resistor and inductor had a big effect on VFTO parameters. Test results revealed that the newly developed simulation system could generate 2.5MV VFTO with a risetime of 49ns and oscillation frequency of 8.1MHz.

2 EXPERIMENTAL ARRANGEMENT

2.1 Generation system of VFTO

Figure 1 shows schematic diagram of VFTO generation system. Impulse voltage generated by the impulse generator(IG) 1 propagates to the first bus 6 through overhead line 2 and HV bushing 3. The bushing and first bus is used to energy storage, which can store the wave front energy of lighting impulse(LI) before breakdown of sharpener gap temporarily. The energy stored is released when sharpener gap breaks down, and then VFTO is generated in test terminal 12. Hemisphere of sharpener gap connected with the first damping resistor 7 is an obturator and is installed with adjustable electrode and gas pipeline. The length of adjustable electrode is controlled by regulating gas pressure through the pipeline outside GIS vessel 4. Therefore the gap clearance and

breakdown voltage are regulated. The method restrains jitter of VFTO when gas switch breaks down and reduces breakdown time dispersion of sharpener gap, which makes the VFTO output more stable. It is worthy to note that the generation system can also generate LI by bridging sharpener gap only, which is convenient to make a comparative research of breakdown characteristics of SF_6 gap under VFTO and LI.

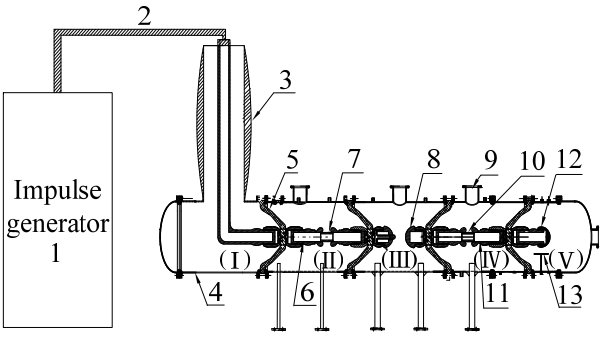

1-impulse generator 2-overhead line 3-HV bushing 4-GIS vessel 5-supporting insulator 6-the first bus 7-the first damping resistor 8-sharpener gap 9-conical voltage sensor 10-the second damping resistor 11-the second bus 12-test terminal 13-plate electrode

Figure 1: Diagram of VFTO generation system.

The parameters of above-mentioned generation system are so huge that makes physical image and concept vague. It's hard to confirm major influence factor on VFTO and guide the design of GIS configuration properly. So, the model of generation system is simplified based on validity and precision. Equivalent inductance of IG is so big that restrains the charge to HV bushing and the first bus at the instant of sharpener gap breaks down. So wave-front of VFTO is mainly determined by ISC C_p(equivalent capacitor of bushing and the first bus) and test capacitor C_t. The equivalent circuit is shown in figure 2.

The Laplace equation of Fig.2 is:

$$\left(\frac{1}{sC_p}-\frac{V_0}{s}\right).I(s)+R.I(s)+Ls.I(s)+\frac{1}{sC_t}.I(s)=0 \qquad (1)$$

where, V_0 is the initial voltage of C_p.

If the current is oscillation waveform, then $R<2\sqrt{L/C}$.

So, the current i(t) is derived:

$$i(t)=\frac{V_0}{\omega L}\mathrm{e}^{-at}\sin\omega t \qquad (2)$$

where:

$$1/C=1/C_p+1/C_t,\ \alpha=R/2L,\ \omega=\sqrt{1/LC-\alpha^2} \qquad (3)$$

If, $\alpha<<\omega$, the voltage u(t) on C_t can be simplified as:

$$u(t)=\frac{V_0C_p}{C_t+C_p}\left(1-\mathrm{e}^{-at}\cos\omega t\right) \qquad (4)$$

The maximum of u(t) can be expressed as:

$$u_{\max}=\frac{V_0C_p}{C_t+C_p}\left(1+\mathrm{e}^{-\frac{a\pi}{\omega}}\right) \qquad (5)$$

The equations mentioned above indicate that frequency, risetime and amplitude of VFTO are determined by circuit parameter *R*,*L* and *C*. It is also worthy to note that the amplitude of VFTO is mainly determined by C_p and C_t because $\alpha<<\omega$.

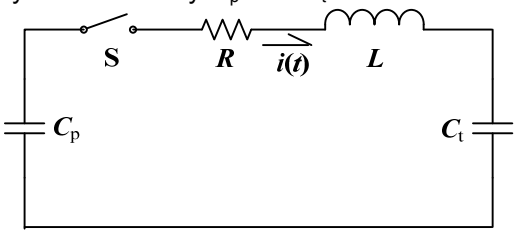

C_p-ISC S-switch gap *R*-circuit equivalent resistance *L*- circuit equivalent inductance *C*-entrance capacitance of test object

Figure 2: Wave-front equivalent circuit.

2.2 Design of Conical Voltage Sensor

Amplitude of VFTO to be measured is several megavolts, which calls for large voltage attenuation ratio of voltage sensor. The low voltage capacitance of conical voltage sensor is larger than traditional plane voltage sensor, so the voltage attenuation ratio is larger, when sensor electrode is the same. Besides, conical structure of voltage sensor realizes smooth transition of wave impedance from high voltage arm to coaxial cable, which drastically reduces refraction and reflection of voltage wave when it propagates in measurement system. So, the conical voltage sensor is chosen as the measurement equipment based on two merits mentioned above.

Sketch map of conical voltage sensor is shown in figure 3. The high voltage capacitor consists of HV bus of GIS, sensor electrode and SF_6 gas between them. The capacitance of high voltage arm is about 0.2pF obtained by calculation. The low dielectric loss of high voltage arm has the merit of short response time, which makes measurement of VFTO with fast risetime more accurate [15].

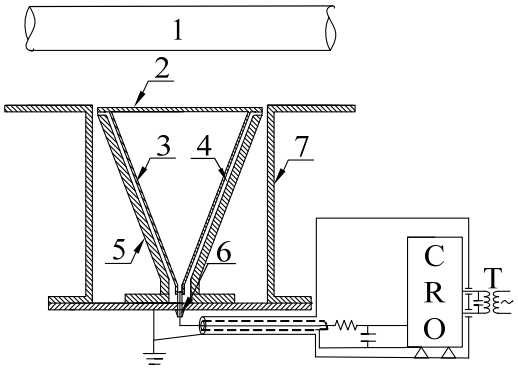

1-HV bus of GIS 2-sensor electrode 3-inner cone 4-PI film 5-outer cone 6-BNC connector 7-ground electrode

Figure 3: Sketch map of conical voltage sensor

A thin polyimide(PI) film of a few microns thickness between inner cone and outer cone made of aluminum is used for dielectric of low voltage arm. The dielectric constant of PI is found to be constant for a wide range of frequencies and is suitable for this application. A thin layer of SF_6 gas in series with PI film makes the capacitance of low voltage arm less than the designed static capacitance[15].

The defect is overcome by coating both sides of PI film with silver paint, which makes a close contact of PI film with inner and outer cone. The capacitance of low voltage arm measured by electric bridge is 9.8nF. The output signal is taken from low voltage capacitor through a conical terminal and transmitted to oscillograph.

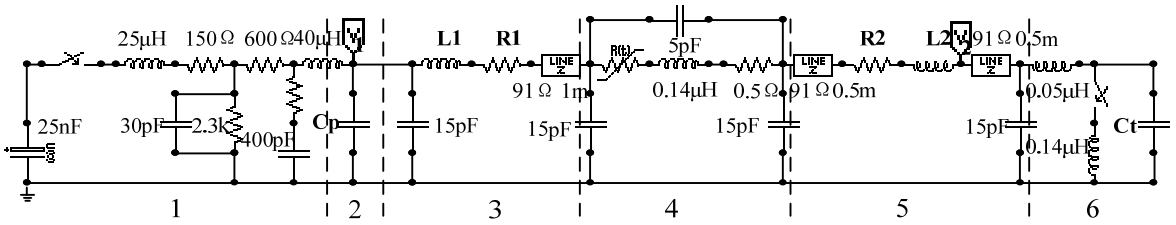

1-impulse generator 2-HV bushing 3-gas vessel II 4-gas vessel III 5-gas vessel IV 6-gas vessel V

Figure 4: Simulation model of VFTO generation system

3 SIMULATION OF GENERATION SYSTEM

Based on current technology and simulation demand, parameters of generation system is primarily selected as: risetime of VFTO<50ns; time to half value:50μs; oscillating frequency: 8~30MHz; amplitude >2.5MV.

The influence of ISC (C_p), circuit inductance and resistance on VFTO parameters are investigated. Simulation model of VFTO generation system is shown in figure 4. Selection of model parameters can refer to literatures[8]. In special, HV bushing is characterized by lumped capacitor and inductor, while HV bus is characterized by distributed parameters. The voltage probe V_1 and V_2 are placed at terminal of HV bushing and measurement point of conical voltage sensor respectively. The time step for simulation is 0.3ns and the total calculation time is 6μs.

Figure 5 shows the VFTO generated by simulation model. It can be seen sharpener gap breaks down near the peek of LI. While voltage measured by V_2 indicated by solid line has a risetime of 49.5ns and oscillating frequency of 8.5 MHz, which reproduces characteristics of fast risetime and high oscillating frequency of VFTO more veritably.

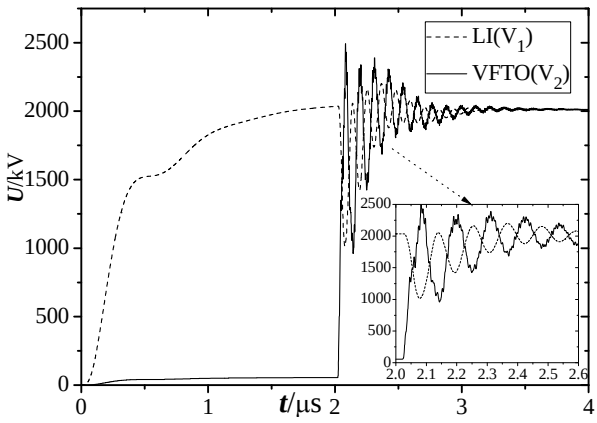

Figure 5: VFTO generated by simulation model

3.1 Effect of ISC on VFTO

Figure 6 shows the effect of ISC on output efficiency and predominant frequency of VFTO.

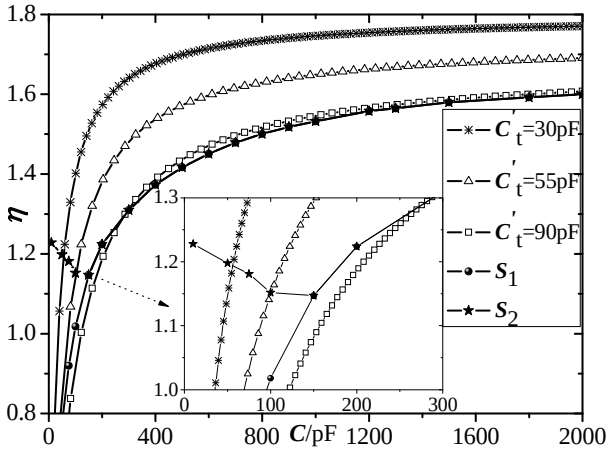

C'_t-equivalent test capacitance S_1- the first peak value of VFTO S_2- peak value of VFTO

(6-a) effect of ISC on output efficiency of VFTO

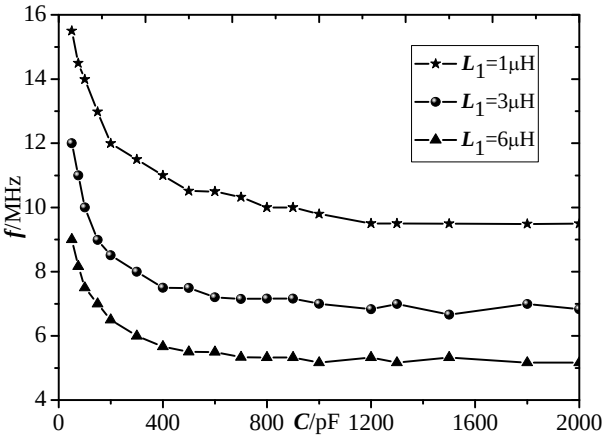

(6-b) effect of ISC on VFTO frequency

Figure 6: Effect of ISC on VFTO parameters

The output efficiency η is defined by the ratio of amplitude of VFTO to value of LI at breakdown time. The equivalent test capacitance (C'_t) includes test capacitance (C_t), capacitance of supporting

insulator and HV bus after V_2, which is about 90pF by calculation. The curves of different C'_t are calculated by formula (4). While S_1 and S_2 are the simulation results of figure 4. It can be deemed from figure 6(a) that the simulation results are highly consistent with calculation results when C'_t is 90pF. It also can be seen from figure 6(b) that frequency of VFTO decreases inversely and trend to constant with increase of C_p.

The change law of figure 6 can be explained by formula (3) and (5).The output efficiency η increases with the increase of C_p and decrease of C_t. Meanwhile, it is interesting to note that η will trends to 2 in condition that C_p trends to infinity and C_t trends to infinitesimal. Further researches reveal that the peak value of VFTO only appears in the first peak as shown in figure 5 when C_p > 150 pF. However, attention also must be paid to the fact that frequency of VFTO decrease sharply with increase of C_p when C_p<400pF. Consequently, C_p is selected as 200pF for a proper high efficiency and frequency.

3.2 Effect of inductance on VFTO

Figure 7 shows the effect of the first damping inductance on risetime and frequency of VFTO. It can be seen that the risetime of VFTO increases with the increase of inductance. By contrast, the predominant frequency of VFTO decreases with the increase of inductance.

It can be deduced from formula (3) that:

$$f = \sqrt{\frac{1}{C}\cdot\frac{1}{L}\cdot-\frac{R^2}{4}\cdot\left(\frac{1}{L}\right)^2} \quad (6)$$

$$t_r \approx 1/4.f \quad (7)$$

It's obvious the change tendency in figure 7 can be seen clearly when R and C are substituted by 45Ω and 200pF in formula (6) respectively. Further researches reveal inductance of generation system should be as low as possible, when $R < \sqrt{2L/C}$, in order to generate VFTO with higher frequency and shorter risetime.

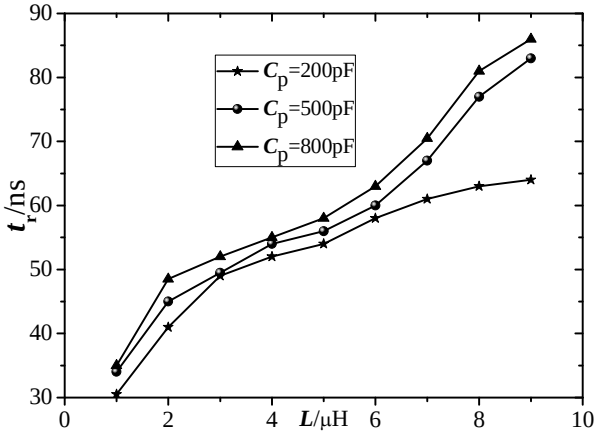

(7-a) effect of inductance on VFTO risetime

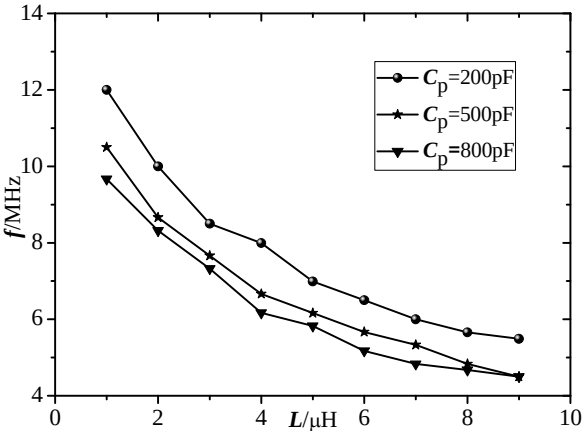

(7-b) effect of inductance on VFTO frequency

Figure 7: Effect of the first damping inductance (L_1) on VFTO parameters

3.3 Effect of resistance on VFTO

Figure 8 shows the effect of damping resistance on amplitude of VFTO. It can be seen that the output efficiency of VFTO increases with the decrease of the first or the second damping resistance. However, the oscillation of VFTO becomes so acute that can't reproduce main characteristics of VFTO properly. Considering this, the first and the second damping resistance are selected as 13Ω and 40Ω respectively.

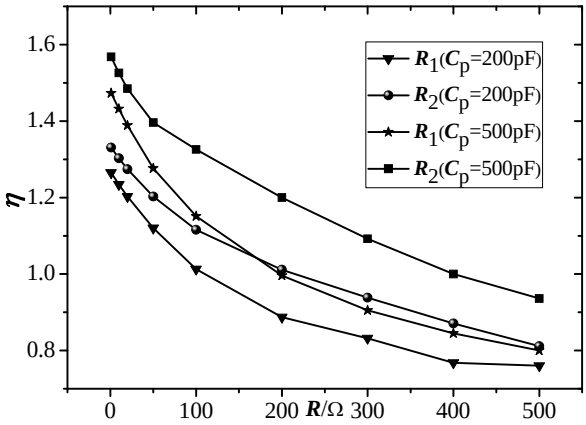

R_1-the first damping resistance R_2-the second damping resistance

Figure 8: Effect of damping resistance on VFTO amplitude

From results mentioned above, three principles in designing VFTO generation systems can be conclude: Firstly, ISC should be selected properly for a higher output efficiency and frequency of VFTO synchronously. Secondly, inductance of generation system must be as low as possible when $R < \sqrt{2L/C}$. Thirdly, a higher efficiency and proper oscillation should be considered in selecting resistance of generation system.

4 MEASUREMENT OF VFTO

4.1 Calibration of Voltage Sensor

High frequency and low frequency response of

conical voltage sensor were calibrated by fast risetime impulse and LI respectively. The impulse was injected from the test terminal. The fast risetime impulse was measured by conical voltage sensor and standard voltage divider simultaneously. While the LI was measured by Tektronix probe P6015 directly. The oscillograph used in experiment is Tektronix DPO4104 (bandwidth : 1GHz, sample rate: 5Gs/s).

The fast risetime impulse was generated by a standard square wave generator, of which the risetime was 3ns and amplitude was adjusted between 0~120kV. Figure 9 shows the response of conical voltage sensor. From figure 9, it can be seen that the risetime of the impulse measured by standard voltage divider and conical voltage sensor are 7.5ns and 8.8ns respectively. The voltage attenuation ratio of the sensor varies between 51835 and 54593 at different voltage levels and the mean value is 53176. The variation range is smaller than 2.6%. It indicates that the newly developed conical voltage sensor can accurately reproduce the fast risetime impulse and has a stable voltage attenuation ratio .

The LI(+1.2/50μs) was generated by a standard LI waveform generator, of which the amplitude was adjusted between 0~5kV. Figure 10 shows the response of conical voltage sensor. It can be seen from figure 10 that the risetime/time to half value of LI measured by Tektronix probe P6015 and conical voltage sensor are 1.53/54.8μs and 1.52/52.7μs respectively. The voltage ratio of the sensor varies between 53414 and 53831 at different voltage levels and the mean value is 53589. The variation range of voltage ratio is smaller than 0.5%. It indicates that the newly developed conical voltage sensor can accurately reproduce the LI. Calibration of voltage sensor under fast risetime impulse and LI shows that the high frequency and low frequency voltage ratio of the sensor is almost the same. The variation range of voltage ratio is smaller than 0.4%. The response time of the sensor is smaller than 10ns and can reproduce nanosecond impulse and LI accurately.

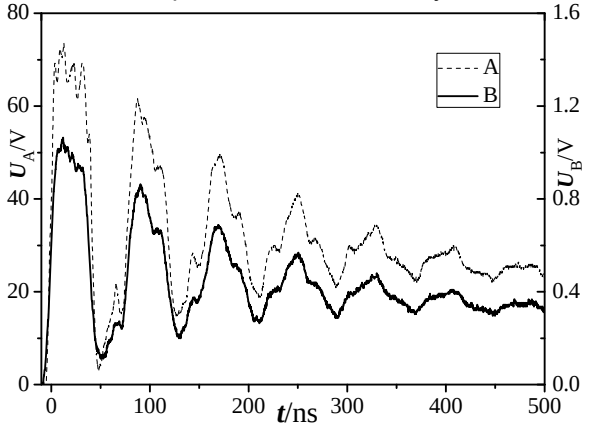

A-resistive voltage divider B-conical voltage sensor
Figure 9: Response of conical voltage sensor excited by fast risetime impulse

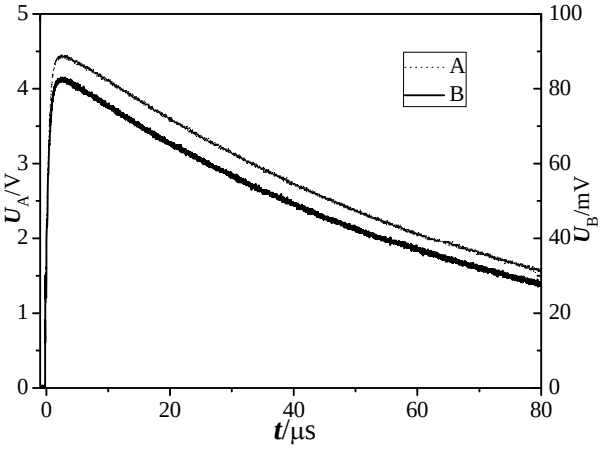

A-Tektronix probe B-conical voltage sensor
Figure 10: Response of conical voltage sensor excited by LI

4.2 Measurement of VFTO in GIS

VFTO measured by conical voltage sensor in the designed generation system is shown in figure 11. LI measured by standard capacitive divider is shown in figure 12.

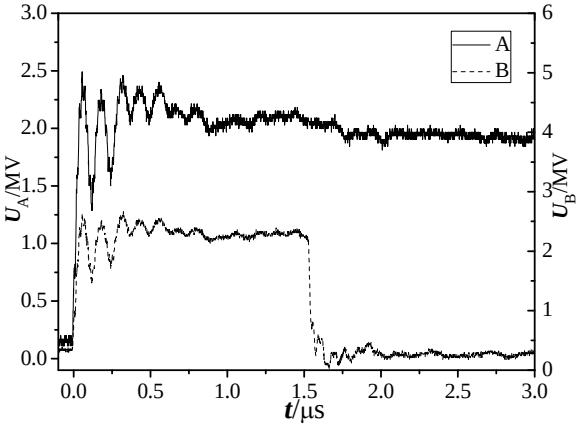

A-full wave B-chopped wave
Figure 11: Output waveform of VFTO measured by conical voltage sensor

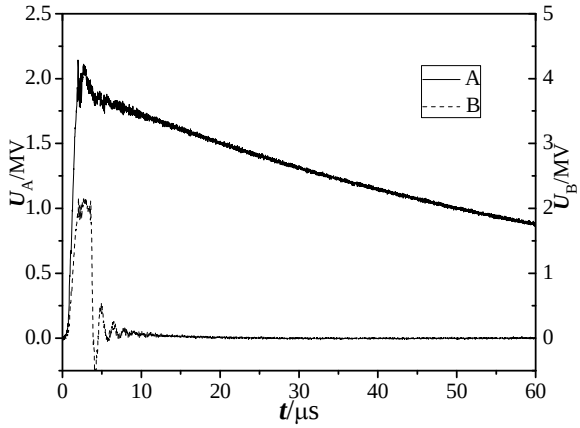

A-full wave B-chopped wave
Figure 12: Output waveform of LI measured by standard capacitive divider

From figure 11-A, it can be seen that the amplitude and risetime of VFTO are 2495kV and 49ns

respectively.The predominant oscillation frequency is 8.1MHz.While the output voltage of IG measured by standard capacitive divider is 2045kV indicated by figure 12-A when the sharpener gap breaks down. So, the output efficiency of VFTO is 1.22.

From the simulation results in figure 4, it can be seen that the amplitude and risetime of VFTO are 2497kV and 49.5ns respectively. The predominant oscillating frequency is 8.5MHz. While the output voltage of IG measured by voltage probe V_1 in figure 4 is 2030kV when the sharpener gap breaks down. So, the simulation results show the output efficiency of VFTO is 1.23. The measurement results are consistent with simulation results.

The above-mentioned results reveal VFTO generated by simulation system can reproduce the main characteristics of VFTO, such as risetime, oscillation frequency and amplitude in actual GIS. So, the generation system can be used to research the insulation characteristics of 1000kV GIS.

5 CONCLUSIONS

To guide the design of 1000kV GIS directly, a new generation system of VFTO was developed to research insulation characteristics of it. The following conclusions can be drawn:

(1) The measurement results are highly in agreement with simulation results. The newly developed generation system can generate 2.5MV VFTO, which has a risetime of 49ns and oscillation frequency of 8.1MHz. It is suitable for researching the insulation characteristics of 1000kV GIS.

(2) The newly developed conical voltage sensor has a wide band and big attenuation ratio, which can accurately reproduce both the low frequency LI and the high frequency VFTO signal with a risetime of several nanoseconds.

(3) *R*, *L*, and *C* of the circuit have an obvious effect on VFTO parameters. Inductance of circuit should be as small as possible, when $R < \sqrt{2L/C}$, for generating VFTO with higher frequency and shorter risetime. A suitable value of damping resistance must be chosen for higher efficiency and proper oscillation of VFTO. It is worthy to note that selection of ISC is related to the value of test capacitance. On precondition of proper frequency, the ISC should be as big as possible for higher output efficiency of VFTO.

6 REFERENCES

[1] Daochun Huang, Yinbiao Shu, Jiangjun Ruan, et al. “Ultra high voltage transmission in China: developments, current status and future prospects”, Pro. of the IEEE, Vol. 97, pp. 555-583, Mar. 2009.

[2] K.D. Srivastava, M.M. Morcos, “A review of some critical aspects of insulation design of GIS/GIL systems”, IEEE/PES T&D Conf. Vol. 1, pp. 787-792**,** Nov. 2001.

[3] Shigemitsu Okabe, Sadayuki Yuasa and Shuhei Kaneko, “Evaluation of breakdown characteristics of gas insulated switchgears for non-standard lightning impulse”, IEEE Trans. Dielectr. Electr. Insul. Vol. 14, pp. 312-320, Apr. 2007.

[4] Q Zhang, F Tao, L Yang, et al. “Influence of waveform on the accumulation of charges along a particle contaminated spacer surface in SF6 stressed by impulse voltage”, J. Phys. D: Appl. Phys. Vol. 38, pp. 1221–1224, 2005.

[5] Santanu Singha and M. Joy Thomas, “Toepler’s spark law in a GIS with compressed SF6-N2 mixture”, IEEE Trans. Dielectr. Electr. Insul. Vol. 10, pp. 498-505, Jun. 2003.

[6] Toshiaki Rokunohe,Toshiyuki Suzuki, Tokio Yamagiwa, et al.“Insulation characteristics of SF6 gas for non-standard impulse voltage polarity reversal pulse waveforms”, Electrical Engineering in Japan, Vol. 146, pp. 1232–1237, Nov. 2004.

[7] Shigemitsu Okabe, Jun Takami and Kenichi Nojima, “Circuit models of gas insulated switchgear elements for electromagnetic wave leakage analysis”, IEEE Trans. Dielectr. Electr. Insul. Vol. 15, pp. 1439-1448, Oct. 2008.

[8] M. Mohana Rao, M. Joy Thomas and B. P. Singh, “Frequency characteristics of very fast transient currents in a 245-kV GIS”, IEEE Trans. Power Del.,Vol. 20, pp. 2450-2457, Oct. 2005.

[9] J. Meppelink, K. Diederich, K. Feser, et al, “Very fast transients in GIS”, IEEE Trans. Power Del., Vol. 10, pp. 223–233, Jan. 1989.

[10] Jose Lopez-Roldan, Terry Irwin, Steve Nurse, et al, “Simulation and testing of an EHV metal-enclosed disconnector”, IEEE Trans. Power Del., Vol. 16, pp. 558-563, Oct. 2001.

[11] V. Vinod Kumar, Joy Thomas M. and M. S. Naidu, “Influence of switching conditions on the VFTO magnitudes in a GIS”, IEEE Trans. Power Del., Vol. 16, pp. 539-544, Oct. 2001.

[12] Shigeto Fujita, Yoshikazu Shibuya and Masaru Ishii, “Influence of VFT on shell-type transformer”, IEEE Trans. Power Del. Vol. 22, pp. 217-222, Jan. 2007.

[13] K. Tekletsadik, L. C. Campbell, “SF6 breakdown in GIS”, IEE Proc.-Sci Meas. Technol., Vol. 143, pp. 270-276, Sep. 1996.

[14] M. Popov, L. van der Sluis, R.P.P. Smeets, “Modelling, simulation and measurement of fast transients in transformer windings with consideration of frequency-dependent losses”, IET Electr. Power Appl., Vol. 1, pp. 29-35, Jan. 2007.

[15] M. Mohan Rao, H.S. Jain, S. Rengarajan, et al, “Measurement of very fast transient overvoltages(VFTO) in a GIS module”, Pro. of 11th ISH, Vol. 1, pp. 1144-1147, Aug. 1999.